Construction and Building Materials 312 (2021) 125397

Contents lists available at ScienceDirect

Construction and Building Materials

journal homepage: www.elsevier.com/locate/conbuildmat

Hybrid cements: Towards their use as alternative and durable materials against wear

S. Shagñay *, A. Bautista, F. Velasco, M. Torres-Carrasco

Materials Science and Engineering Department-IAAB, University Carlos III of Madrid, Avda. Universidad 30, 28911 Leganés, Madrid, Spain

ARTICLE INFO

Keywords:
Construction materials
Hybrid materials
Abrasive wear
Durability

ABSTRACT

Hybrid cements (HC) are a possible replacement of Portland cement, as their activation process only requires a small amount of sulphates, and is carried out with water at room temperature. The present work aims to study the wear behaviour of HC manufactured from two different wastes: blast furnace slag (HS) and fly ash (HFA). Their wear behaviour was compared to Portland cements (CEM I and CEM IV). Reciprocating wear tests and rolling wear Böhme tests were carried out for pastes and mortars, respectively. Wear tracks in the pastes were analysed through opto-digital microscopy and electron microscopy (SEM). In the mortars, the mechanical resistance was measured to understand different behaviours.

The results obtained reveal that HC pastes and mortars present lower wear losses than CEM IV and similar to CEM I.

1. Introduction

Portland cement is essential in construction. It is the second most used material in the world after water. The global cement production in 2018 was 4.2 Gt, according to the World Cement Association (WCA), and it is expected to remain flat until 2030. Moreover, WCA reports that cement accounts for 2.5 Gt of CO_2 emissions, about 7% of the world's total. The Green Growth and Sustainable Development Forum organized in November 2019 by the Organisation for Economic Co-operation and Development (OECD) concluded that cement and concrete represent 6% of global energy system combustion and industrial process CO_2 emissions [1,2].

The cement industry is working to develop sustainable cements, reducing its clinker content, which is a short-term strategy to lower the CO_2 emissions of existing plants [1], as is also established by the Global Cement and Concrete Association. Alkali-activated materials (AAM) or geopolymers -whose performance can match or even exceed ordinary Portland cements (OPC) thanks to their physical–chemical properties- [3-5] constitute an interesting alternative based on industrial wastes, such as fly ash [6,7] or blast furnace slag [8]. However, these wastes are aluminosilicates and need alkaline activators to be useful products, like NaOH or sodium silicate, among others [9,10]. There are some environmental drawbacks related to the fly-ash and slag activation process. By way of comparison between Portland cement and AAM production, the CO_2 emissions generated are around 354 kg CO_2/m^3 and 320 kg CO_2/m^3, respectively [11]. The CO_2 emissions produced in AAM are related to the production of the activators used (silicate or sodium hydroxide, for instance). These alkaline solutions are harmful from an environmental point of view, so attempts have been made to search for other alternatives, such as the use of waste glass to produce activators that are an alternative to sodium silicate [3,12,13]. In addition, the difficulty of preparing large volumes of alkaline solutions is a significant obstacle for the upscaling of AAM. Moreover, for the activation of fly ash, thermal curing is necessary to favour the precipitation of zeolites that are the precursors of sodium aluminosilicate hydrate (N-A-S-H) gel, the main reaction product, which is another clear drawback for its in-construction use [14,15]. For these reasons, up to now, AAM has been exclusively processed in an extensive way for prefabricated materials, and, if AAM were to be generalized for use in civil construction, it would lead to serious problems. In addition, AAM present other drawbacks such as issues related to high shrinkage and subsequent formation of microcracks, rapid setting, formation of salt efflorescence and expansive reactions due to alkali-aggregate reactions [16,17].

Nowadays, there are alternative routes to reducing contamination from processing alkaline products, as hybrid cements (HC). HC are mixtures of 70–80% fly ash or blast furnace slag with 30–20% OPC [18,19]. These mixtures require 3–5% Na_2SO_4 -either liquid or solid- as activators, and can be hydrated at room temperature simply with water

* Corresponding author.
E-mail address: sshagnay@ing.uc3m.es (S. Shagñay).

https://doi.org/10.1016/j.conbuildmat.2021.125397
Received 20 April 2021; Received in revised form 3 September 2021; Accepted 24 October 2021
Available online 3 November 2021

additions [20,21]. For that reason, these alternative materials can be produced on a large scale in the construction industry. Fig. 1 shows the range of compositions for these kinds of materials in comparison to OPC.

The difference between the properties of the OPC, AAM and HC materials is related to the main reaction products formed. The main product reaction is calcium silicate hydrate (C-S-H gel) in OPC systems. Portlandite and ettringite, among other secondary reaction products, are also formed, such as [22-24]. The activation of AAM with a high calcium content (such as blast furnace slag) promotes a calcium aluminosilicate hydrate gel (C-(A)-S-H gel) as its main product, while an amorphous alkali aluminosilicate (N-A-S-H gel) is found in with low calcium content AAM (such as fly ash) [4,25-28]. However, in the case of HC, there is a complex mix of gels, such as C-S-H gel and N-(C)-A-S-H (a calcium-substituted N-A-S-H), which eventually evolves into a more thermodynamically stable C-A-S-H gel [29,30]. This is due to the presence of Portland cement in the system (around 20–30%) as well as different industrial wastes (70–80%).

Millan-Corrales et al. [21] and Qu et al. [31] have shown that HC with maximum 20–30% OPC, based on blast furnace slag or fly ash, and low content (3–5%) of solid activator present good mechanical resistance at room and high temperatures, even better than CEM I Portland cement and AAM. In general, the HC have received extensive interest because of their high temperature resistance, low permeability, good durability and environment friendliness. Furthermore, these cements show good early age mechanical development. Palomo et al. [18] have determined that this good resistance at early ages is attributed to the formation of mixture of gels. Martauz et al. [32] studied shrinkage of hybrid mortars and determined that they have a lower shrinkage in comparison to AAM.

From the point of view of durability, wear and/or abrasion resistances of construction materials are of great interest. The wear behaviour is important for understanding problems such as the wear of surfaces (floors or slabs), or surface problems due to percussion, scratching and attrition from automobiles and heavy trucks. Railroad ties made of AAM with blast furnace slag can suffer erosion, although no wear tests were carried out [33,34]. In fact, there are very few published studies in this regard on AAM and there is hardly any information on HC systems. Shagñay et al. [35] studied the wear behaviour of AAM pastes, and determined that AAM with blast furnace slag has better wear behaviour than AAM with fly ash and CEM IV.

The present study aims to manufacture and study pastes and mortars of HC composed of either fly ash or blast furnace slag mixed with Portland CEM I and activated with Na_2SO_4 (hybrid materials), using only water as the hydrating product, in order to evaluate their wear performance, and using different tests for pastes and mortars.

2. Experimental procedure

2.1. Materials

Two commercial Portland cements (CEM I and CEM IV/B) were used. An F-type fly ash furnished by the Puentenuevo steam plant in the Spanish province of Cordoba and blast furnace slag provided by the Aviles factory (Spain) were also used. Table 1 shows their chemical composition determined by X-ray fluorescence spectroscopy with a Spectro Xepos III X-ray spectrometer.

2.2. Pastes and mortars preparation

CEM I and CEM IV pastes and mortars were prepared as well as HC systems mixing fly ash and slag with 20% (by wt.) of CEM I, as can be seen in Table 2. Furthermore, Na_2SO_4 was used as the solid alkaline activator for both HC, hybrid blast furnace slag (HS) and hybrid fly ash (HFA), at different percentages (3% and 5% of Na_2SO_4), according to previous work [21,31]. The liquid/solid ratio (L/S) for all systems was determined according to EN 196–3 standard, with water used in all cases. Mortar samples were prepared with standard sand with 0.08–2 mm of grain size as EN 196–1 recommends. All systems were chamber-cured above 90% relative humidity at room temperature for 2, 7, and 28 days. All pastes and mortars were treated with acetone/ethanol to stop hydration/activation and kept in the desiccator at 0% relative humidity until evaluation of their properties. Later, during testing, the relative humidity of the laboratories, is not higher than 20%. Table 2 summarises the manufactured materials.

2.3. Tests conducted

For the cured materials, pore size distribution and total porosity were measuring by Hg intrusion porosimetry, using a Micrometrics AUTO-Pore IV 9500 analyser.

Stiffness (YHU) and universal hardness (HU) were determined [36], following the advices of EN ISO 14577–1 standard. A 10 N load was used on pastes, with 3 mm/min of application speed and 5 mm/min of removal speed. A Zwick/Roell ZHU 2.5 universal hardness tester was used. The stiffness of the material was obtained during the unloading (load removal) stage.

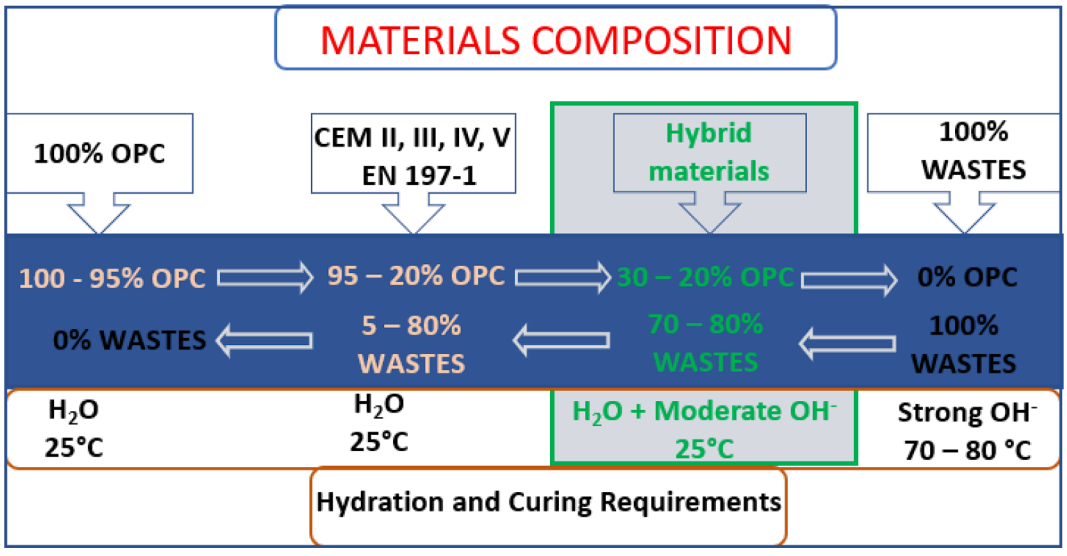

Fig. 1. Classification of materials with respect to their composition.

Table 1
Chemical composition of used materials (% by wt.).

wt%	CaO	SiO_2	Al_2O_3	MgO	Fe_2O_3	SO_3	K_2O	TiO_2	*L.O.I.
CEM I	61.0	20.9	6.3	<0.01	2.5	5.8	1.0	0.2	2.35
CEM IV	33.3	48.0	13.0	1.7	5.3	3.4	1.4	0.4	3.50
Slag	37.4	34.4	11.4	11.7	0.2	1.9	0.3	0.5	2.10
Fly ash	4.0	46.3	28.2	0.6	16.9	1.2	1.1	0.8	1.00

*L.O.I.: loss of ignition.

Table 2
Pastes and mortars prepared and activation condition.

Sample	Composition (wt%)	L/S	
		Pastes	Mortars
CEM I	100	0.35	0.50
CEM IV	100	0.35	0.50
HS	80 Slag + 20 CEM I + 5 Na_2SO_4	0.30	0.42
HFA	80 Fly Ash + 20 CEM I + 3 Na_2SO_4	0.30	0.37

Mechanical behaviour of mortars after 28 days of curing was determined using a Microtest universal testing machine. Three samples of each mortar (CEM I, CEM IV, HFA and HS) were averaged.

The reciprocating wear tests in pastes were carried out with an UMT-TriboLab equipment. The test was developed under dry condition. The applied load was 10 N, against a 6 mm diameter polished Al_2O_3 ball (with ± 2.5 μm tolerance) located above the sample, at room temperature, with a reciprocal movement. Other wear test conditions were: frequency 5 Hz, duration of test 15 min, and wear track amplitude 5 mm. Three tests, for each condition, were performed in each paste sample. The parameters of the reciprocating wear test were determined according to previous works [35]. The morphology and volume of the wear track was characterized by an opto-digital Olympus DSX500 microscope. The lost volume was estimated according to the procedure used by Doni et al. [37] and Shagñay et al. [35]. Furthermore, the Olympus DSX500 microscope was used to determine the initial roughness, measured on an area of 4000 μm^2. The microstructure characterization of the pastes and the wear tracks was carried out using a TENEO FEI scanning electron microscope (SEM). Before their observation, the samples were kept at 80 °C for 30 min, and then were covered with graphite paint to get a high vacuum.

Böhme machine abrasive test in mortars was carried out according to UNE-EN 13892–3 standard under an applied load of 294 N. Brown fused alumina (aluminium oxide) was used as abrasive material. Three tests, for each mortar, were performed at 16 test cycles, each consisting of 22 revolutions. Wear was determined by equation (1) after 16 cycles in the same sample according to UNE-EN 13892–3 standard.

$$A = \Delta V = \frac{\Delta m}{\rho} = \Delta l \times 5 \left[cm^3 \ per \ 50 \ cm^2\right] \quad (1)$$

where ΔV is the total volume lost in cm^3 after 16 cycles, Δm is the mass lost after 16 cycles, Δl is the thickness lost after 16 cycles, and ρ is the mortar density. Wear data were obtained from thickness loss measurements.

The use of different types of wear test for mortars and pastes is due to absence of sand in the latter materials. Reciprocating tests allow a first knowing of wear mechanisms of the pastes of the different materials under study. Böhme is much more aggressive as it is specifically designed for materials with aggregates.

3. Results and discussion

3.1. Pastes and mortars: Physical and mechanical properties

Fig. 2 shows the porosities of the pastes measured for the three curing times considered in this study. For all pastes, the porosity decreases with curing time, as expected (Fig. 2). The different setting reactions (depending on the specific paste) promote this effect, as the formed gels close porosity. At 28 curing days, hybrid slag pastes exhibit the lowest porosity. On the other hand, CEM IV pastes show the highest porosity at any of the studied curing times. This porosity should exert a strong influence on mechanical and tribological properties, with better properties expected for less porous materials. The distribution of porosity can also play a role in the durability of pastes. Pore size distributions (Fig. 2) of all pastes show a reduction of bigger pores with curing time, which can be clearly related to the formation of gels. This effect is particularly important for CEM I (with the formation of C-S-H gel) and HS (C-A-S-H gel) [29,30], where more than half of pores after 28 days are smaller than 0.1 μm. The fly ash (present in HFA) and the natural pozzolanas (in CEM IV) do not promote pore size reduction during the formation of N-A-S-H gel in HFA and C-S-H gel in CEM IV. The anhydrous fly ashes used have a particle size smaller than 45 μm. With this size, they are not able to fill any pore in the cementicious material, thus not affecting pore size.

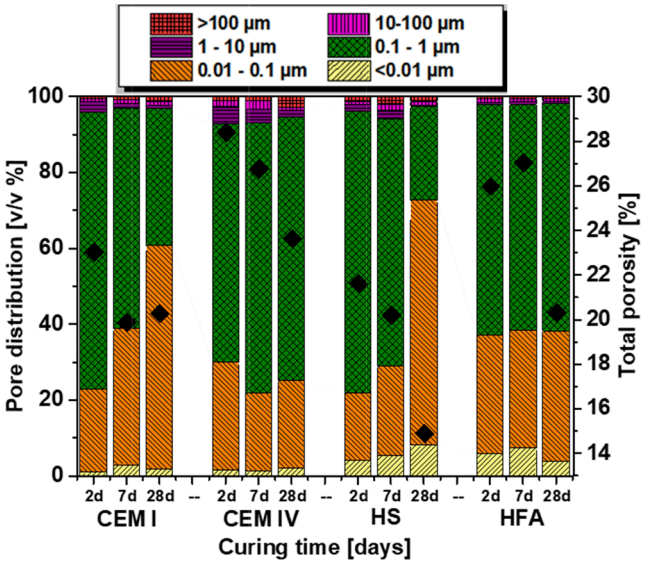

Fig. 2. Total porosity of pastes and their pore size distribution.

Total values of porosity of mortars (Fig. 3) are smaller than those of pastes. As sand present in mortars has no pores, this reduction is obvious. Porosity of mortars comes from that of pastes (Fig. 2) and from possible pores in the paste-sand interface [38]. Pore size distributions in mortars (Fig. 3) clearly show an increase in pore size, with it being noticeable that there is a greater number of pores that are bigger than 1 μm, due to the presence of fine aggregates [39]. Having a high binder/sand ratio (1/3), dense slurry is formed with aggregate and binder particles uniformly distributed and surrounded by water.

The effect of curing reactions on porosity also affects the mechanical properties of pastes and mortars. It is particularly interesting to study the mechanical performance of new HC materials to understand their possible effect on wear properties. Fig. 4a shows the hardness of the different studied pastes at different ages, with it being possible to observe that this property increases with curing time. The reduction of

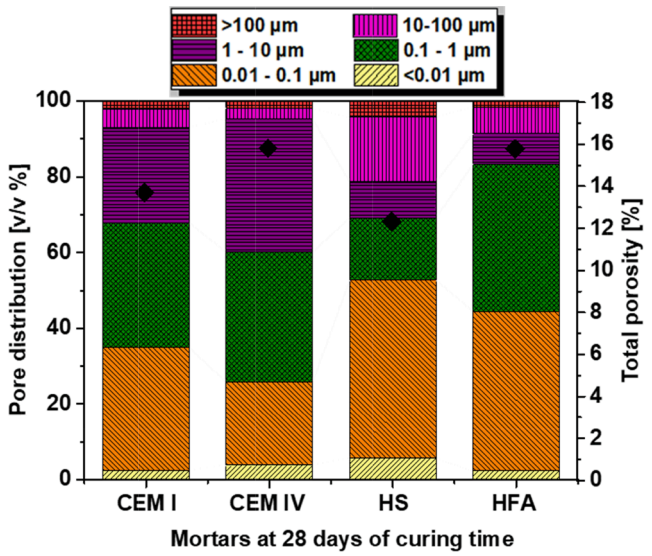

Fig. 3. Total porosity of mortars (cured for 28 days) and their pore size distribution.

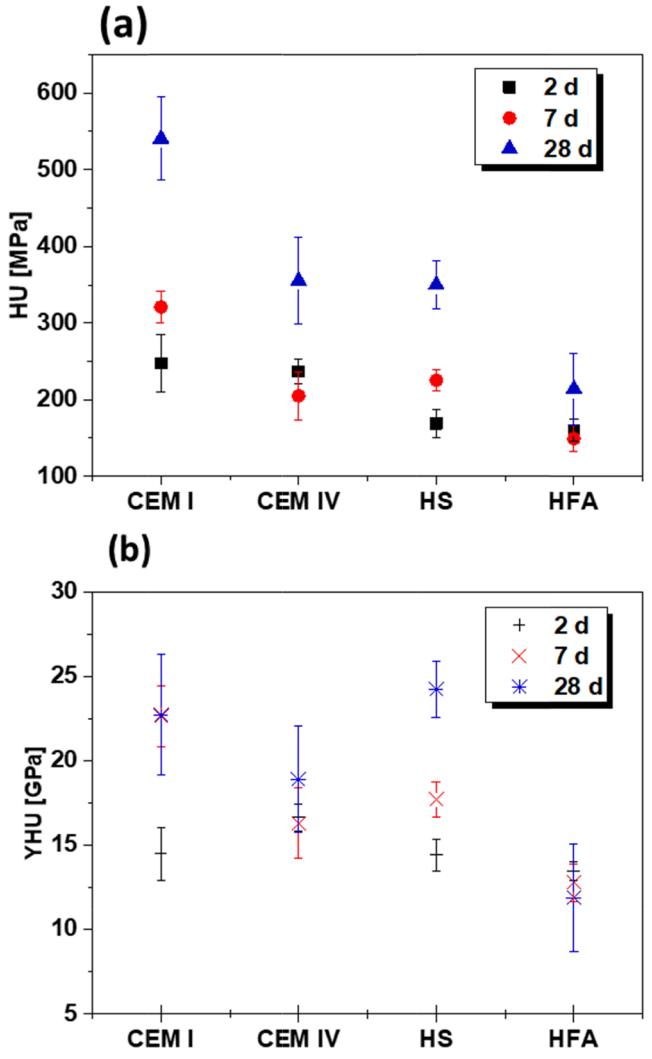

Fig. 4. a) Universal hardness (HU) and b) stiffness (YHU) of the different pastes under study.

porosity (Fig. 2) and the closing of the biggest pores due to the formation of gels promote the well-known hardening of cement-based pastes [40-42]. The values of hardness, however, are not easily related to those of porosity. The nature of formed gels clearly plays a dramatic role in the final hardness of pastes (Fig. 4a). CEM I presents the highest hardness values, as it is almost pure clinker cement (>95%), with a very high amount of C-S-H gel. It is remarkable that HS pastes present hardness similar to CEM IV pastes. CEM IV has a content of 45–64% clinker, while manufactured HS has 20% CEM I, clearly indicating the ability of slag to form gels in the HS formulation.

The positive effect of densification of HS pastes can be seen in the stiffness of pastes (Fig. 4b), showing average values similar to that of CEM I, whose structure is clearly harder. On the other hand, the higher porosity (Fig. 2) and the lower hardness of HFA gels make this paste the one with the lowest stiffness.

As can be seen in Fig. 5, as hydration evolves over time, the surface average roughness (S_a) of the pastes also increases due to their low consistency. The HS and HFA pastes exhibit the lowest roughness with respect to CEM IV systems over time (7 and 28 days). It is important to highlight that HS and HFA pastes exhibit sulphate content on the surface from the beginning (at short curing time), [16]. The presence of these sulphates increases the surface roughness. As curing proceeds, roughness might directly affect the wear behaviour, as there are slight differences between pastes with different compositions for the same curing time.

The mechanical behaviour of the mortars studied after 2, 7 and 28 curing days is shown in Fig. 6. At 28 days of curing time the HS (41 MPa) presents higher values of compression strength than HFA (22 MPa), and even more than CEM IV reference mortar (29 MPa). In addition, HS mortars have a resistance similar to that of CEM I mortars. This higher compression strength of CEM I (42 MPa) is related to its high clinker content (95–100%) according to UNE-EN 197–1, but the gels formed in HS can offer a similar compression resistance which a clicker content of only 20%. In any event, the sand and its bonding play a very important role in mortar strength. Due to its size and shape, sand can have better bonding with irregular particles such as the slag particles and contribute to the good compression properties exhibited by HS mortars.

In Fig. 7, representative SEM images of the pastes of the different systems evaluated can be seen. At the shown magnification, both CEM I (Fig. 7a) and CEM IV (Fig. 7b) pastes show smooth-textured hydration products, where complete hydration has taken place, in accordance with strength values (Fig. 6). These flat grains are separated from each other by a porous mass of finer hydrated components with a less homogeneous appearance. The aspect of HS paste (Fig. 7c) is similar to CEM I and CEM

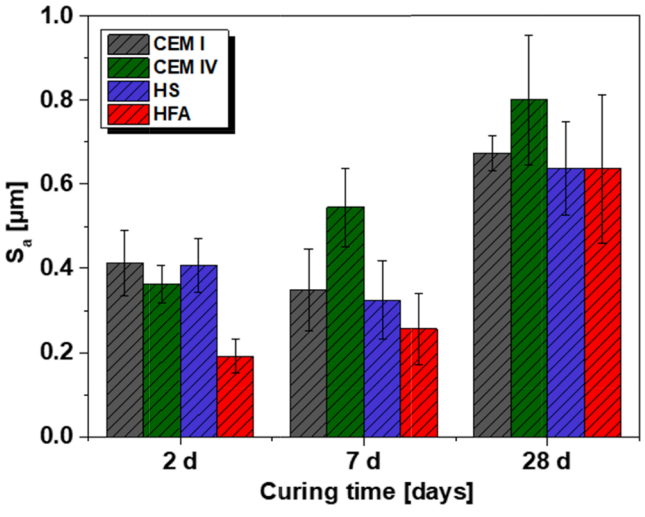

Fig. 5. Surface average roughness (S_a) of the pastes studied after different curing times.

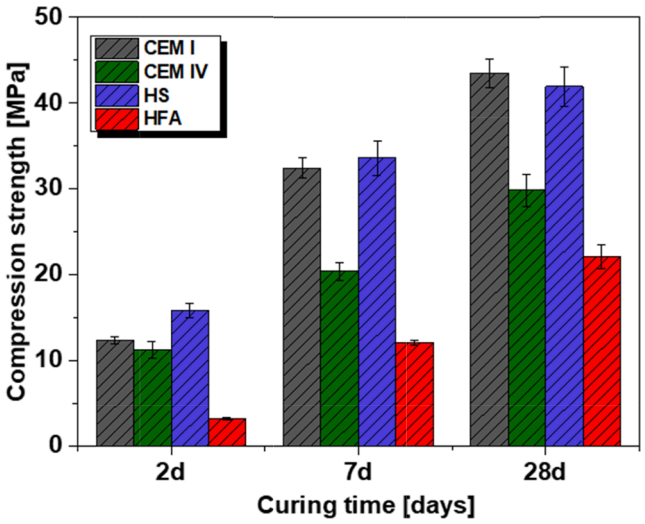

Fig. 6. Compression strength of the different mortars studied.

IV, although the regions with fine reacted products seem denser, as porosity (Fig. 2) suggests. Some cracks appear on HS, clearly related to shrinkage during setting. Activated slag cement shrinkage is larger than that of Portland cement, thus promoting this effect on studied hybrid cements [43]. On the other hand, HFA material (Fig. 7d) shows spherical fly-ash particles that have not reacted with the activator. Then, they do not form zeolites, that are the precursors for N-A-S-H gel, explaining porosity results (Fig. 2), together with their particle size. These spheres will present low adherence with sand particles causing not enough gel formation in the interface between them and the sand [14], playing an important role in the mechanical behaviour of the HFA mortars.

3.2. Wear behaviour in pastes

Pastes are very important for understanding many factors about the resistance of the reaction products of the different materials under study. Fig. 8 shows the monitored coefficient of friction over time obtained during some of the reciprocating-slide wear tests carried out for 2 and 28-days cured pastes.

In all the cases but CEM I and IV after 2 days of curing, the coefficient of friction is more or less constant during the wear tests, with this

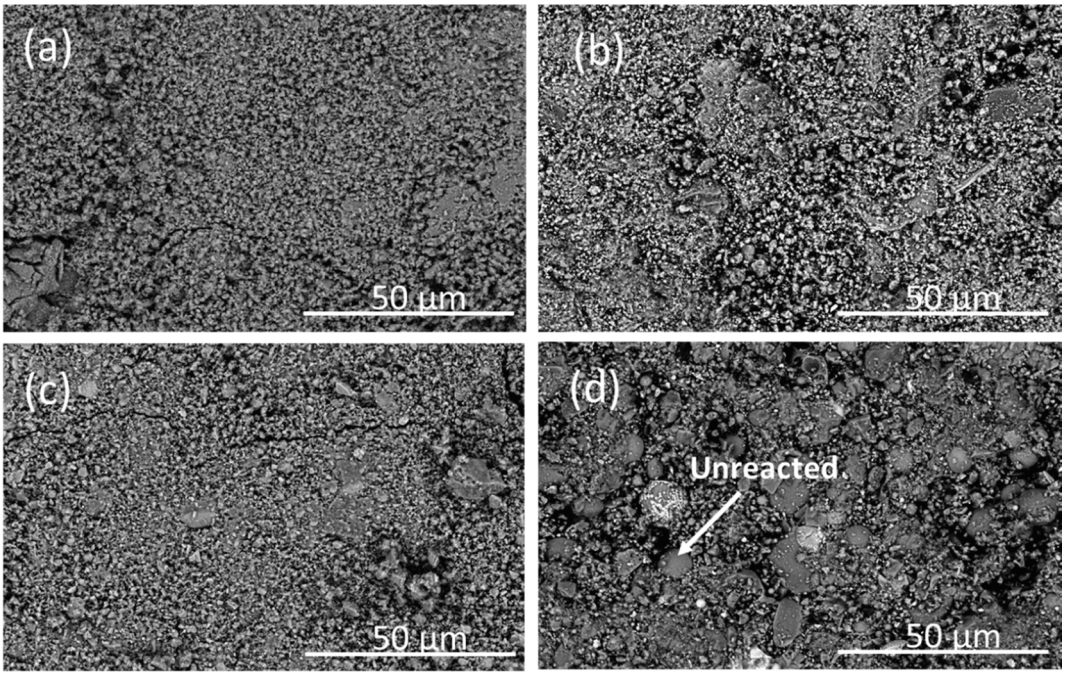

Fig. 7. SEM images of representative areas of pastes cured for 28 days: a) CEM I; b) CEM IV; c) HS; and d) HFA.

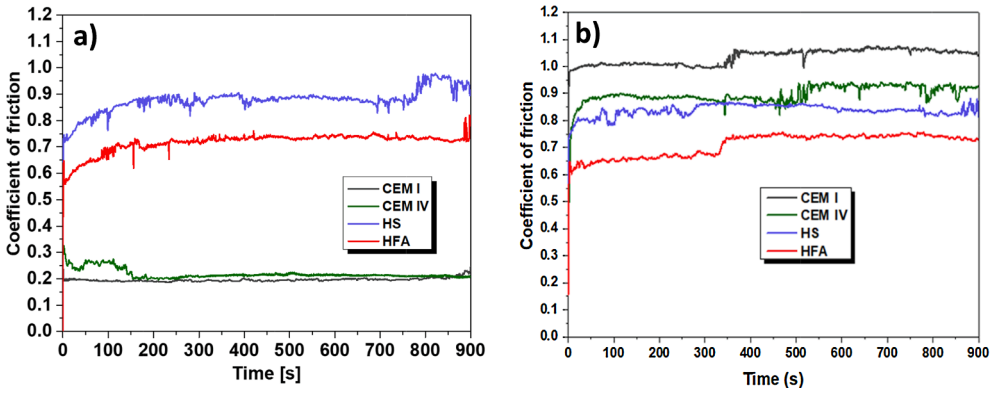

Fig. 8. Coefficient of friction for all the studied pastes cured for a) 2 and b) 28 days.

behaviour comparable to those shown in other studies in similar systems [35,44]. The wear tracks have been formed from the beginning of the test (t = 0), due to the friction between the surface of the pastes and the countermaterial (Al_2O_3). As no low friction coefficient region appears at the beginning of the tests, no sliding takes place between alumina and studied pastes (Fig. 8). The coefficient of friction reaches values of about 0.7 or higher very quickly, without major variations of the coefficient of friction during the rest of the test. The high friction coefficients during tests suggest an abrasive wear mechanism [45].

On the other hand, the two OPCs (CEM I and CEM IV) cured for 2 days show a different behaviour. The coefficient of friction stays low during the entire test (Fig. 8a), with values of approximately 0.2. This is typical of the sliding performance, which can be related to the ratio L/S 0.35 (CEM I and CEM IV) that it is higher than HS and HFA (Table 2). As a consequence, a surface layer can be seen with a high water concentration.

Wear behaviour of the pastes is directly related to hardness, porosity, and stiffness of the materials (Figs. 2 and 4). In this study, coefficient of friction of HFA pastes is 0.7 approximately, being the lowest of all the 28-days cured pastes.

On the other hand, measurements of the coefficient of friction using nano-scratch have shown that microporosity of pastes can increase the coefficient of friction, as the indenter could plough deeper into the matrix [46], as they affect both hardness and stiffness. In the present research, no predominant effect of any parameter has been found.

Fig. 9 shows examples of 3D images of representative wear tracks, after the reciprocating wear test for all 28-days cured pastes. Differences in the depth and width of the wear tracks due to the composition of the pastes can be seen in Fig. 9. The change in these dimensions is used for calculating the volume losses plotted in Fig. 10.

It can be appreciated that HS pastes present the smallest and least deep wear track (Fig. 9c) after 28 days of curing, with both being plain Portland cements (Fig. 9a and b) very similar. Fig. 9d shows that the HFA wear track is the widest and the deepest among studied pastes. These observations lead to results in Fig. 10, where HS pastes cured for 28 days present the lowest average volume loss after wear test, although differences with CEM I and CEM IV are not significant. The wear behaviour of HS hybrid pastes, with only 20% CEM I in their composition, is as good as the two tested OPCs, with this environmentally-friendly material being a good option for wear applications. In this case, the volume loss of the HS can be clearly related to the low roughness and high stiffness and hardness (Figs. 4 and 5) of these pastes. The positive effect of Na_2SO_4 as an activator, when reacting with CEM I, promotes mixed C-S-H and C-A-S-H gels and secondary reaction products, which can greatly decrease porosity (Fig. 2) and increase hardness and stiffness (Fig. 5), thereby improving the wear behaviour. The

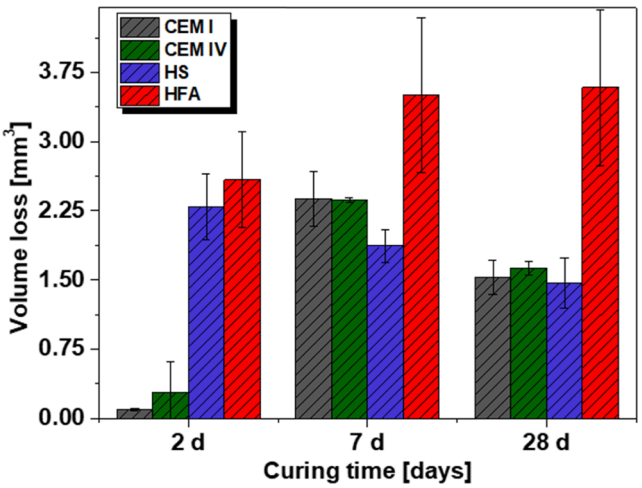

Fig. 10. Volume loss of pastes after wear test.

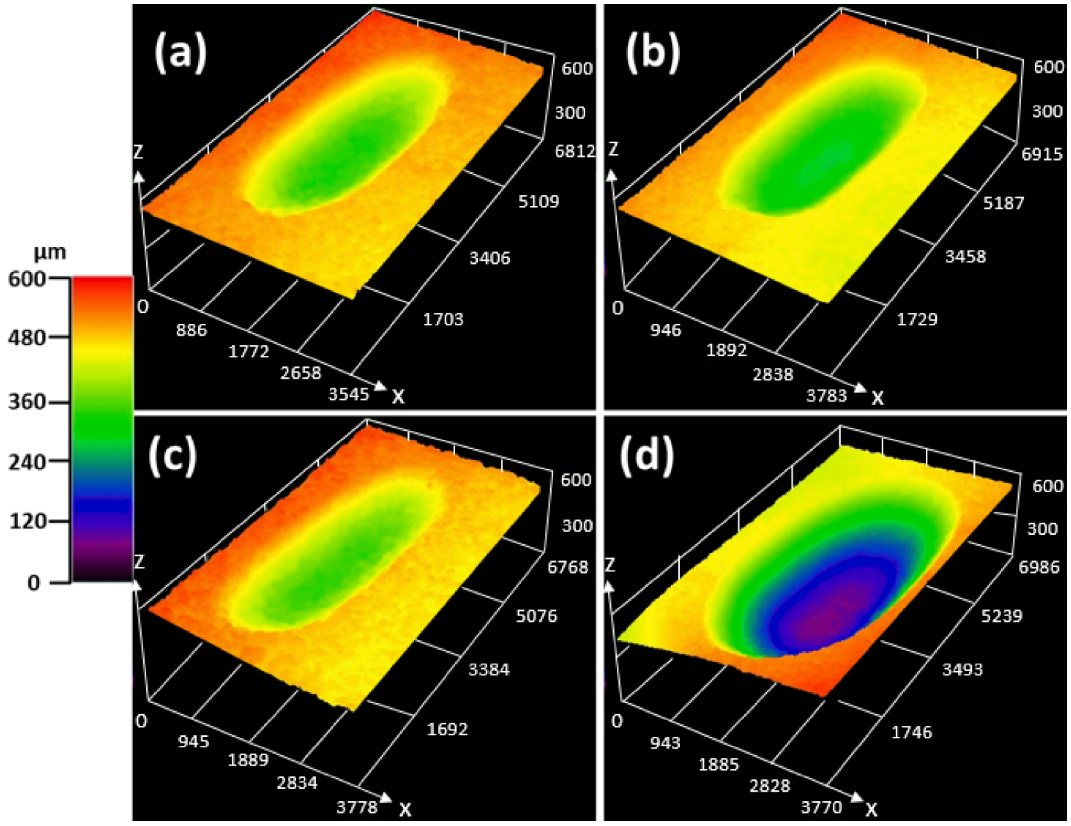

Fig. 9. 3D opto-digital images of representative wear tracks at 28 days of curing of: a) CEM I, b) CEM IV, c) HS, d) HFA. All units in images are µm.

evolution of wear losses of pastes with curing time is coherent with coefficient of friction data and the properties of the materials. CEM I and CEM IV cured for 2 days, where sliding takes place (Fig. 8a), present very shallow wear tracks and wear losses are very low (as can be clearly appreciated in Fig. 10) due to the presence of moisture on the tested surface. In addition, the increase of hardness and stiffness (Fig. 5) and the reduction of porosity (Fig. 2) with curing time make the materials more wear resistant, as the formation of C-S-H and C-A-S-H gels takes place over time.

On the other hand, HFA pastes experience high wear, even though they have the lowest coefficient of friction (Fig. 8), as previously shown for plain fly-ash pastes [35]. HFA pastes exhibit not fully reacted ash particles, generating a more porous material with low hardness and stiffness (Fig. 4) that present worse wear behaviour, more than doubling the volume losses of the other pastes (Fig. 10).

However, it is important to highlight that 28 days are required to complete hydration processes, and the study of wear results at this time is the most adequate.

In Fig. 11, representative SEM images of the middle of the wear tracks of the different systems evaluated can be seen. After the wear test, CEM I clearly shows flattening in the worn surface and there are no scratches (Fig. 11a). The removed material in CEM I seems to be related to very fine hydrated products, which are more abundant in the surface. The wear track in CEM IV (Fig. 11b) shows areas with cracks and flattening on all the surface due to abrasion between the base material and countermaterial. White areas could correspond to non-hydrated material [47], which do not appear in CEM I. This could explain the lower hardness and stiffness together with the typical additions of CEM IV (the presence of a high percentage of additions in its composition, such as fly ash and slags that do not exist in CEM I). The wear tracks in HS pastes (Fig. 11c) predominantly show material loosening of the fine reacted grains, as no large hydrated grains are found in the structure (Fig. 7c). However, as already mentioned in Fig. 7c and 7d, there are unreacted slag and fly ash particles (non-hydrated materials). No scratches, typical of an abrasive wear mechanism, are found (Fig. 11c) in any of those three materials. However, different behaviour can be observed for HFA pastes (Fig. 11d). During the wear test, in this case, many microcracks are generated in the surface as well as flattening. Moreover, abrasion in this less hard and stiff material (Fig. 5) due to its lower curing promotes a global abrasion with lower forces required to remove material (Fig. 8).

To obtain more information about how abrasion can affect the pastes, SEM compositional maps were made and the qualitative elementary composition was obtained around the interface between base material (bm) and wear track (wt). Fig. 12 shows that there are differences between the chemical composition of base material and wear track for all pastes. Fig. 12a and 12b, corresponding to mortars manufactured from commercial cements clearly show changes in the Ca and Si content, as can be seen in the colour variation due to the chemical composition of both cements (see Table 1).

On the other hand, HC pastes show an important difference in sulphur content. During manufacturing of the pastes, the sulphur from the Na_2SO_4 tends to migrate to the external surface due to the effect of efflorescence [16]. As in the track, the outer layer is erased by wear, and an increase on Ca content is observed.

3.3. *Influence of fine aggregates on wear performance of hybrid mortars: Böhme test*

In this research, information about the wear performance of the pastes has been complemented with that of mortars to identify the effect of additions of fine aggregates. Fig. 13 shows volume losses after abrasion Böhme wear test of all mortars after different curing periods.

Mortars cured up to 28 days have the lowest volume losses (Fig. 13) due to the formed reaction products. The effect of curing time on the increase in the compression strength (Fig. 6) of materials clearly improves their abrasion performance. This parallelism between strength and abrasion agrees with the general trend, where increasing the strength of concrete reduces the effects of abrasion [48,49].

However, the differences found among mortars for compression resistance (Fig. 6) are lower than those found for wear results (Fig. 13). As Böhme is an abrasion test, sand withstands most of the stresses (all materials have the same amount of fine aggregate). For instance, HFA

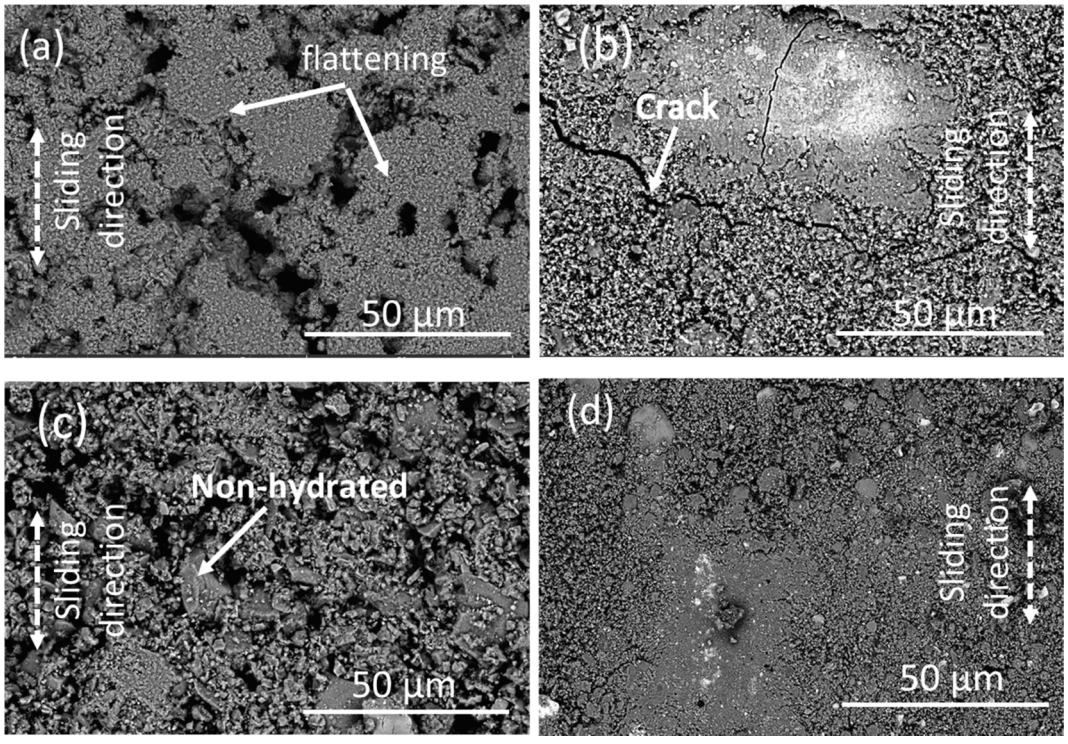

Fig. 11. SEM images of the middle of the wear tracks in pastes cured for 28 days: a) CEM I; b) CEM IV; c) HS; and d) HFA.

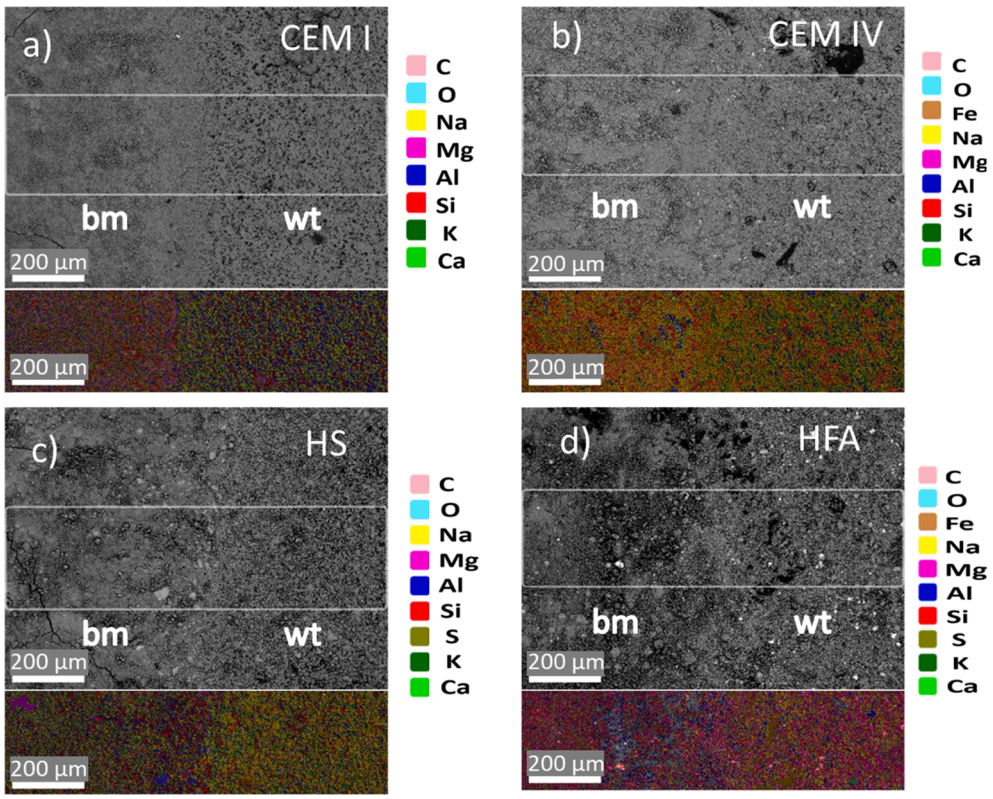

Fig. 12. SEM compositional maps in the interface between base material (bm) and wear track (wt). a) CEM I, b) CEM IV, c) HS and d) HFA.

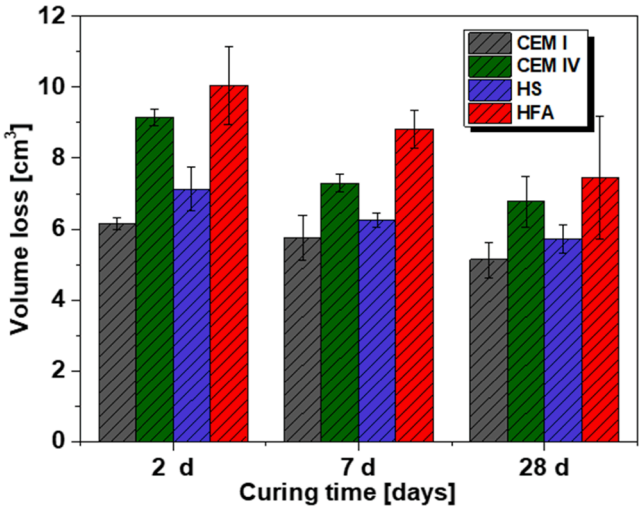

Fig. 13. Volume loss after abrasive wear test (Böhme) of mortars.

mortar shows half the compression strength of CEM I and HS, and more than double the wear losses in the reciprocal tests where only paste is considered (Fig. 10). Moreover, the adherence of the sand to the matrix is another key point for stress distribution and for keeping the sand grains attached to the mortar and protecting it instead of becoming an additional aggressive third body in the test. The sand-matrix adhesion obviously influences the compression tests but was more of a determining factor for abrasive wear conditions. The adherence of the sand is clearly related to the porosity formed in the sand-gels interface and to their bonding ability.

Besides the different tests used, the sand-matrix bonding ability is a key factor for understating how pastes whose formulations do not show any noticeable difference in their wear resistance (Fig. 9) can exhibit relevant differences when they are manufactured as mortars. The reduced porosity of the HS mortars (Fig. 3) allows their wear resistance to be higher than that of CEM IV (Fig. 13) in spite of the similar hardness for both pastes (Fig. 4). Moreover, it should be highlighted that the wear performance of HS is similar or only slightly lower than that of highly contaminant CEM I (Fig. 13) mortar. Although the HS pastes are not as hard as CEM I are (Fig. 4a), the low porosity of HS must promote an increased sand-matrix adherence and favours the durability of the material under abrasive conditions.

AAM have already been carefully used as eco-friendly alternative to OPC cements in modern airports as those of Brisbane West Wellcamp (Australia), in the turning node, apron and taxiway pavements or all the heavy duty pavements in aircraft turning areas at Toowoomba Wellcamp (Australia). Their mechanical performance complies with all the requirements without problems. However, the cost related to the activators [50] is a clear drawback for a wider implementation. The good wear behaviour of HS opens the way for application of these new eco-friendly, easily-activated materials, such as on highways, runways at airports submitted to wear efforts, as well as for the manufacture of construction materials such as blocks or paving stones. For other applications where cement is extensively used, but the small shrinkage problems detected in the present research could affect the in-service performance, as structures summitted to fatigue or efforts, further research must be conducted and the addition of anti-shrinkage additives, for instance. This a subject the authors are presently studying. For reinforced concrete structures, the chemical protection given to the steel for HS concretes in environments with chlorides and with risk of carbonation of leaching would be explored in further works of the authors.

4. Conclusions

In this work, hybrid material pastes and mortars were used to study wear behaviour. After carrying out this research, the following main

conclusions can be drawn:

- Hybrid mortars and pastes have been manufactured from slag and fly ash using only 20% clinker and an easily in-construction implementable activation process. The hybrid materials manufactured for slag (HS) have shown reduced porosity in comparison with those manufactured from traditional CEM I and IV.
- Gels formed on HS pastes after 28 days of curing have shown hardness similar to those from CEM IV and stiffness that is even similar to those from CEM I pastes.
- HS mortar shows compression strengths higher than those from CEM IV and similar to those of CEM I after 7 and 28 days of curing.
- The wear performance of all the pastes studied takes place under an abrasive mechanism during reciprocating sliding tests. The volume losses after 28 days of curing are similar for all the pastes, except for HFA, where unreacted fly-ash particles worsen the behavior.
- The good sand-matrix adherence of the HS mortars (related to their porosity) promotes a high abrasive wear resistance, higher than that of CEM IV and quite similar to that of CEM I mortars.

CRediT authorship contribution statement

S. Shagñay: Conceptualization, Methodology, Formal analysis, Investigation, Resources, Data curation, Writing – original draft, Visualization. **A. Baustista:** Conceptualization, Formal analysis, Funding acquisition, Investigation, Methodology, Resources, Writing – original draft, Supervision. **F. Velasco:** Conceptualization, Formal analysis, Funding acquisition, Methodology, Resources, Writing – review & editing, Supervision, Project administration. **M. Torres-Carrasco:** Conceptualization, Formal analysis, Funding acquisition, Investigation, Methodology, Resources, Writing – original draft, Supervision.

Declaration of Competing Interest

The authors declare that they have no known competing financial interests or personal relationships that could have appeared to influence the work reported in this paper.

Acknowledgements

This work has been supported by the Madrid Government (Comunidad de Madrid) under the Multiannual Agreement with UC3M in the line of “Fostering Young Doctors Research” (HORATSO-CM-UC3M) in the context of the V PRICIT (Regional Programme of Research and Technological Innovation), and by the Ministerio de Ciencia, Innovación y Universidades of Spain through project RTI2018-096428-B-I00.

References

[1] C. Bataille, Low and zero emissions in the steel and cement industries, in: Green Growth Sustain. Dev. Forum, Paris, 2007, pp. 1–41.
[2] M.R. Karim, H. Hashim, H. Abdul Razak, S. Yusoff, Characterization of palm oil clinker powder for utilization in cement-based applications, Constr. Build. Mater. 135 (2017) 21–29, https://doi.org/10.1016/J.CONBUILDMAT.2016.12.158.
[3] F. Puertas, M. Torres-Carrasco, Use of glass waste as an activator in the preparation of alkali-activated slag. Mechanical strength and paste characterisation, Cem. Concr. Res. 57 (2014) 95–104, https://doi.org/10.1016/j.cemconres.2013.12.005.
[4] M. Torres-Carrasco, F. Puertas, La activación alcalina de diferentes aluminosilicatos como una alternativa al Cemento Portland: cementos activados alcalinamente o geopolímeros, Rev. Ing. Constr. 32 (2017) 5–12, https://doi.org/10.4067/s0718-50732017000200001.
[5] Y. Tajunnisa, R. Bayuaji, N.A. Husin, Y.N. Wibowo, M. Shigeishi, Characterization Alkali-Activated Mortar Made From Fly Ash And Sandblasting, Int. J. GEOMATE. 17 (2019) 183–189, https://doi.org/10.21660/2019.60.24636.
[6] A. Fernández-Jiménez, A. Palomo, Characterisation of fly ashes. Potential reactivity as alkaline cements, Fuel 82 (18) (2003) 2259–2265, https://doi.org/10.1016/S0016-2361(03)00194-7.
[7] W.K. Part, M. Ramli, C.B. Cheah, An overview on the influence of various factors on the properties of geopolymer concrete derived from industrial by-products, Constr. Build. Mater. 77 (2015) 370–395, https://doi.org/10.1016/J.CONBUILDMAT.2014.12.065.
[8] S.-D. Wang, K.L. Scrivener, Hydration products of alkali activated slag cement, Cem. Concr. Res. 25 (3) (1995) 561–571, https://doi.org/10.1016/0008-8846(95)00045-E.
[9] D. Dimas, I. Giannopoulou, D. Panias, Polymerization in sodium silicate solutions: A fundamental process in geopolymerization technology, J. Mater. Sci. 44 (14) (2009) 3719–3730, https://doi.org/10.1007/s10853-009-3497-5.
[10] K.-H. Yang, J.-K. Song, A.F. Ashour, E.-T. Lee, Properties of cementless mortars activated by sodium silicate, Constr. Build. Mater. 22 (9) (2008) 1981–1989, https://doi.org/10.1016/j.conbuildmat.2007.07.003.
[11] L.K. Turner, F.G. Collins, Carbon dioxide equivalent (CO2-e) emissions: A comparison between geopolymer and OPC cement concrete, Constr. Build. Mater. 43 (2013) 125–130, https://doi.org/10.1016/j.conbuildmat.2013.01.023.
[12] M. Torres-Carrasco, J.G. Palomo, F. Puertas, Sodium silicate solutions from dissolution of glasswastes. Statistical analysis, Mater. Constr. 64 (314) (2014) e014, https://doi.org/10.3989/mc.2014.v64.i314.
[13] M. Torres-Carrasco, C. Rodríguez-Puertas, M.D.M. Alonso, F. Puertas, Alkali activated slag cements using waste glass as alternative activators. Rheological behaviour, Bol. La Soc. Esp. Ceram. y Vidr. 54 (2) (2015) 45–57, https://doi.org/10.1016/j.bsecv.2015.03.004.
[14] A. Fernández-Jiménez, A. Palomo, M. Criado, Microstructure development of alkali-activated fly ash cement: A descriptive model, Cem. Concr. Res. 35 (6) (2005) 1204–1209, https://doi.org/10.1016/j.cemconres.2004.08.021.
[15] Z. Xie, Y. Xi, Hardening mechanisms of an alkaline-activated class F fly ash, Cem. Concr. Res. 31 (9) (2001) 1245–1249, https://doi.org/10.1016/S0008-8846(01)00571-3.
[16] A. Fernández-Jiménez, J.G. Palomo, F. Puertas, Alkali-activated slag mortars: Mechanical strength behaviour, Cem. Concr. Res. 29 (8) (1999) 1313–1321, https://doi.org/10.1016/S0008-8846(99)00154-4.
[17] M. Torres-carrasco, A. Campo, M.A. De Rubia, E. Reyes, A. Moragues, J. F. Fernández, New insights in weathering analysis of anhydrous cements by using high spectral and spatial resolution Confocal Raman Microscopy, Cem. Concr. Res. 100 (2017) 119–128, https://doi.org/10.1016/j.cemconres.2017.06.003.
[18] Á. Palomo, O. Maltseva, I. García-Lodeiro, A. Fernández-Jiménez, Hybrid alkaline cements. Part II: The clinker factor, Rev. Rom. Mater. Rom. J. Mater. 43 (2013) 74–80.
[19] I. García-Lodeiro, O. Maltseva, Á. Palomo, A. Fernández-Jiménez, Hybrid alkaline cements. Part I: Fundamentals, Rev. Rom. Mater. Rom. J. Mater. 42 (2012) 330–335.
[20] B. Lothenbach, K. Scrivener, R.D. Hooton, Supplementary cementitious materials, Cem. Concr. Res. 41 (12) (2011) 1244–1256, https://doi.org/10.1016/j.cemconres.2010.12.001.
[21] G. Millán-Corrales, J.R. González-López, A. Palomo, A. Fernandez-Jiménez, Replacing fly ash with limestone dust in hybrid cements, Constr. Build. Mater. 243 (2020) 118169, https://doi.org/10.1016/j.conbuildmat.2020.118169.
[22] M. Torres-Carrasco, A. Campo, M.A. Rubia, E. Reyes, A. Moragues, J.F. Fernández, In situ full view of the Portland cement hydration by confocal Raman microscopy, J. Raman Spectrosc. 50 (5) (2019) 720–730, https://doi.org/10.1002/jrs.v50.510.1002/jrs.5574.
[23] E. L'Hôpital, B. Lothenbach, K. Scrivener, D.A. Kulik, Alkali uptake in calcium alumina silicate hydrate (C-A-S-H), Cem. Concr. Res. 85 (2016) 122–136, https://doi.org/10.1016/J.CEMCONRES.2016.03.009.
[24] I.G. Richardson, The calcium silicate hydrates, Cem. Concr. Res. 38 (2) (2008) 137–158, https://doi.org/10.1016/j.cemconres.2007.11.005.
[25] I. Garcia-Lodeiro, A. Palomo, A. Fernández-Jiménez, An overview of the chemistry of alkali-activated cement-based binders, Handb. Alkali-Activated Cem. Mortars Concr. (2014) 19–47, https://doi.org/10.1533/9781782422884.1.19.
[26] M. Torres-Carrasco, F. Puertas, Waste glass in the geopolymer preparation. Mechanical and microstructural characterisation, J. Clean. Prod. 90 (2015) 397–408, https://doi.org/10.1016/j.jclepro.2014.11.074.
[27] E. Altan, S.T. Erdoğan, Alkali activation of a slag at ambient and elevated temperatures, Cem. Concr. Compos. 34 (2) (2012) 131–139, https://doi.org/10.1016/j.cemconcomp.2011.08.003.
[28] S. Alonso, T. Va, F. Puertas, S. Martō, Alkali-activated fly ash / slag cement Strength behaviour and hydration products, Cem. Concr. Res. 30 (2000) 1625–1632, https://doi.org/10.1016/S0008-8846(00)00298-2.
[29] J.F. Rivera, R.M. De Gutierrez, J.M. Mejia, M. Gordillo, Hybrid cement based on the alkali activation of by-products of coal, Rev. La Constr. 13 (2014) 31–39, https://doi.org/10.4067/s0718-915x2014000200004.
[30] I. Garcia-Lodeiro, A. Fernandez-Jimenez, A. Palomo, Hydration kinetics in hybrid binders: Early reaction stages, Cem. Concr. Compos. 39 (2013) 82–92, https://doi.org/10.1016/j.cemconcomp.2013.03.025.
[31] B. Qu, A. Fernández Jiménez, A. Palomo, A. Martin, J.Y. Pastor, Effect of high temperatures on the mechanical behaviour of hybrid cement, Mater. Construcción. 70 (337) (2020) 213, https://doi.org/10.3989/mc.2020.v70.i33710.3989/mc.2020.13318.
[32] P. Martauz, I. Janotka, J. Strigác, Fundamental properties of industrial hybrid cement : utilization in ready-mixed concretes and shrinkage-reducing applications, Mater. Constr. 66 (2016), e084, https://doi.org/10.3989/mc.2016.04615.
[33] R. Sañudo, M. Miranda, C. García, D. García-Sanchez, Drainage in railways, Constr. Build. Mater. 210 (2019) 391–412, https://doi.org/10.1016/j.conbuildmat.2019.03.104.
[34] M. Shojaei, K. Behfarnia, R. Mohebi, Application of alkali-activated slag concrete in railway sleepers, Mater. Des. 69 (2015) 89–95, https://doi.org/10.1016/j.matdes.2014.12.051.

[35] S. Shagñay, F. Velasco, A. del Campo, M. Torres-Carrasco, Wear behavior in pastes of alkali-activated materials: Influence of precursor and alkali solution, Tribol. Int. 147 (2020) 106293, https://doi.org/10.1016/j.triboint.2020.106293.
[36] W.C. Oliver, G.M. Pharr, Measurement of hardness and elastic modulus by instrumented indentation: Advances in understanding and refinements to methodology, J. Mater. Res. 19 (1) (2004) 3–20, https://doi.org/10.1557/jmr.2004.19.1.3.
[37] Z. Doni, A.C. Alves, F. Toptan, J.R. Gomes, A. Ramalho, M. Buciumeanu, L. Palaghian, F.S. Silva, Dry sliding and tribocorrosion behaviour of hot pressed CoCrMo biomedical alloy as compared with the cast CoCrMo and Ti6Al4V alloys, Mater. Des. 52 (2013) 47–57, https://doi.org/10.1016/j.matdes.2013.05.032.
[38] J. Elsen, C. Groot, in: Characterisation of Old Mortars with Respect to their Repair - Final Report of RILEM TC 167-COM, 2017, https://doi.org/10.1617/2912143675.006.
[39] V.G. Haach, G. Vasconcelos, P.B. Lourenço, Influence of aggregates grading and water/cement ratio in workability and hardened properties of mortars, Constr. Build. Mater. 25 (6) (2011) 2980–2987, https://doi.org/10.1016/j.conbuildmat.2010.11.011.
[40] F. Kontoleontos, P. Tsakiridis, A. Marinos, N. Katsiotis, V. Kaloidas, M. Katsioti, Dry-grinded ultrafine cements hydration. Physicochemical and microstructural characterization, Mater. Res. 16 (2013) 404–416, https://doi.org/10.1590/S1516-14392013005000014.
[41] P.D. Tennis, H.M. Jennings, Model for two types of calcium silicate hydrate in the microstructure of Portland cement pastes, Cem. Concr. Res. 30 (2000) 855–863, https://doi.org/10.1016/S0008-8846(00)00257-X.
[42] A. Fernández-Jiménez, I. Garcia-Lodeiro, O. Maltseva, A. Palomo, Hydration mechanisms of hybrid cements as a function of the way of addition of chemicals, J. Am. Ceram. Soc. 102 (1) (2019) 427–436, https://doi.org/10.1111/jace:2019.102.issue-110.1111/jace:15939.
[43] A.A. Melo Neto, M.A. Cincotto, W. Repette, Drying and autogenous shrinkage of pastes and mortars with activated slag cement, Cem. Concr. Res. 38 (4) (2008) 565–574, https://doi.org/10.1016/j.cemconres.2007.11.002.
[44] M. Fernández-Álvarez, F. Velasco, A. Bautista, F.C.M. Lobo, E.M. Fernandes, R. L. Reis, Manufacturing and characterization of coatings from polyamide powders functionalized with nanosilica, Polymers (Basel). 12 (2020) 1–20, https://doi.org/10.3390/polym12102298.
[45] S. Affatato, D. Brando, Introduction to wear phenomena of orthopaedic implants, Wear Orthop, Implant. Artif. Joints. (2013) 3–26, https://doi.org/10.1533/9780857096128.1.3.
[46] J. Xu, W.u. Yao, Nano-scratch as a new tool for assessing the nano-tribological behavior of cement composite, Mater. Struct. Constr. 44 (9) (2011) 1703–1711, https://doi.org/10.1617/s11527-011-9728-7.
[47] S. Diamond, The microstructure of cement paste and concrete - A visual primer, Cem. Concr. Compos. 26 (8) (2004) 919–933, https://doi.org/10.1016/j.cemconcomp.2004.02.028.
[48] Y.-W. Liu, T. Yen, T.-H. Hsu, Abrasion erosion of concrete by water-borne sand, Cem. Concr. Res. 36 (10) (2006) 1814–1820, https://doi.org/10.1016/j.cemconres.2005.03.018.
[49] M. Safiuddin, B. Scott, Abrasion resistance of concrete–Design, construction and case study, Concr. Res. Lett. 6 (2015) 136–148.
[50] Z. Abdollahnejad, F. Pacheco-Torgal, T. Félix, W. Tahri, J. Barroso Aguiar, Mix design, properties and cost analysis of fly ash-based geopolymer foam, Constr. Build. Mater. 80 (2015) 18–30, https://doi.org/10.1016/j.conbuildmat.2015.01.063.